

Probing near-surface nanoscale mechanical properties of low modulus materials using a quartz crystal resonator atomic force microscope

This article has been downloaded from IOPscience. Please scroll down to see the full text article.

2011 Nanotechnology 22 295709

(<http://iopscience.iop.org/0957-4484/22/29/295709>)

View [the table of contents for this issue](#), or go to the [journal homepage](#) for more

Download details:

IP Address: 130.209.6.41

The article was downloaded on 05/04/2012 at 15:46

Please note that [terms and conditions apply](#).

Probing near-surface nanoscale mechanical properties of low modulus materials using a quartz crystal resonator atomic force microscope

Yen Peng Kong¹, Ling Chen¹ and Albert F Yee²

Department of Chemical Engineering and Materials Science, University of California, Irvine, CA 92697-2575, USA

E-mail: yenkong@umich.edu, lc43@zips.uakron.edu and afyee@uci.edu

Received 22 February 2011, in final form 24 May 2011

Published 20 June 2011

Online at stacks.iop.org/Nano/22/295709

Abstract

We describe the development of a technique for making indentations on the top 5–20 nm of the surfaces of relatively low modulus materials using a high spatial and force sensitivity atomic force microscope (AFM) whose optical cantilever has been replaced by a quartz crystal resonator (QCR). Unlike conventional optical-cantilever-based AFMs, the accuracy of this technique is not compromised by the compliance of the loading system due to the high stiffness of the QCR. To obtain material modulus values from the indentation results, we find the commonly used Oliver–Pharr model to be unsuitable because of our use of a sharp tip and relatively deep indentation. Instead, we develop a new analysis that may be more appropriate for the geometry we use as well as the non-linear constitutive behavior exhibited by the materials we examined. We calculated values for the moduli of several different materials, which we find to be consistent with the range of published data.

1. Introduction

Knowledge of the surface mechanical properties of materials is important for understanding adhesion, friction and wear, and environmental resistance. Features or structures on the nanometer scale are expected to exhibit size-dependent mechanical properties as the surface-to-volume ratio increases with decreasing feature size. Understanding the mechanical behavior and effect of surfaces on the deformation mechanism of nanostructures will provide the knowledge for designing more robust and stable micro- and nanostructures.

Nanostructures can be fabricated from a variety of materials. Those from polymers are of special interest because polymers can be readily dissolved or melted, or cross-linked from liquid precursors, making them particularly desirable for processing into nanostructures. If desired, these polymeric nanostructures can also serve as the template or underlying

structure for the deposition of other materials such as metals and semiconductors. Yet, the very ease of fabrication into nanostructures gives rise to questions about the subsequent stability of polymeric nanostructures especially when the surface-to-volume ratio becomes significant.

Ceramics and metals, because of their strong bonding, are expected to have a very thin surface zone and so near-surface and bulk mechanical properties may not be very different. Soft materials such as polymers, by contrast, are expected to exhibit significant differences between surface and bulk properties because of the weak secondary bonding in such materials. Furthermore, the long chain nature of polymers means that there may be a significant concentration of chain segments and chain ends in the vacuum half space. Thus, the surface zone in soft materials such as polymers could be at least several molecular diameters thick, i.e. in the order of a few nanometers. Indeed, some measurements of T_g s of ultrathin films of polymers show that they are significantly lower than those of the bulk [1–3]. But polymer chains in

¹ Kong and Chen had equal contributions to this work.

² Author to whom any correspondence should be addressed.

ultrathin films may be biaxially oriented in the plane of the film due to the initial processing, and the resulting anisotropy in entropic force may affect the mechanical properties of the thin film, especially at temperatures near the T_g . Consequently it may not be appropriate or feasible to extrapolate ultrathin film results to polymer surfaces. In this paper we describe a new instrument capable of characterizing the mechanical properties of polymer nanostructures by means of nm-sized indentations and compression. The nm-sized scanning probe we describe avoids the major pitfalls in typical scanning probe measurements of mechanical properties of soft material surfaces. We caution here that our experiments were conducted in air, and therefore surface contamination must be assumed to have contributed to the quantities that we measure.

Nanoindentation instruments have been developed and commercialized to measure the mechanical properties of the near-surface of materials. Unfortunately, the widely used commercial nanoindentation instruments are typically not designed to measure mechanical properties at the scale of interest in this work. Instead, they are typically used to assess near-surface mechanical properties with indentation depths ranging from tens of nanometers to several microns. In addition, the radii of indenters most commonly used are generally on the micron scale or just below, which makes it impossible to resolve features and properties at the nanometer scale. In short, the spatial resolution and force sensitivity of conventional nanoindenters are not appropriate for assessing the characteristics of materials on the scale of a few tens of nanometers and below. AFM based nanoindentation tests have been described in a few publications, which show that the results obtained on metals and other hard materials resemble those obtained on bulk materials [4]. The advantage of using a conventional AFM with an optical cantilever for nanoindentation is the high spatial and force resolution. However, such an instrument has an inherent drawback when used to assess the mechanical properties of soft materials. To measure the very small forces generated by extremely small indentations, the use of very compliant AFM cantilevers is necessary. When indenting a soft material, the cantilever deflection has contributions from both the indenting force and the deformation of the specimen. It is difficult to separate these two contributions. This convolution eventually leads to erroneous estimates of the Young's modulus of surfaces. The uncertainty is especially acute if the surface layer of the specimen is soft relative to the bulk. Additionally, most AFMs use a tilted cantilever setup. This may result in additional lateral force and inaccurate estimation of the contact area due to bending of the cantilever. Thus it is necessary to apply corrections to obtain accurate force measurements when using a conventional AFM for nanoindentation [5]. To assess the mechanical properties accurately, an ideal nanoindenter should have high sensitivity and low compliance. In addition, the axis of the indenting tip should be perpendicular to the sample surface.

In the instrument described in this work, an AFM using a quartz crystal resonator (QCR) as the force sensor mounted in line with the displacement driver is used to satisfy the criteria of low compliance and the ability to vertically position

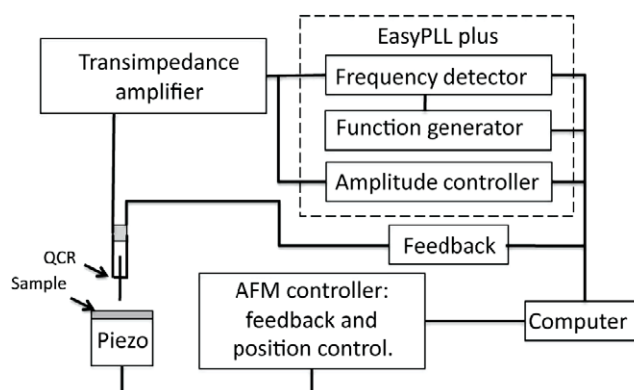


Figure 1. Block diagram of the QCR-AFM instrument.

the indenting tip. The QCR is operated in frequency-modulation (FM-AFM) mode, and the change in vibration frequency as the probe tip contacts the surface can be used to measure the indentation force. To use the QCR FM-AFM as a nanoindentation instrument, the relationship between the applied force and the corresponding change in frequency needs to be established. Theoretical models based on simple harmonic oscillators (SHO) have been developed to relate the applied force to the frequency change [6–10]. Additional theoretical and experimental work have shown that the applied force is linearly proportional to the frequency change at small forces [11–13]. This simple linear relationship makes it possible to calibrate a QCR and use it as a force sensor. In this work, we describe the calibration of the QCR and its use for nanoindentation studies.

2. Instrumentation and experiments

The AFM system used in this study was based on an NTEGRA Therna platform manufactured by NT-MDT. Frequency modulation was provided by the 'EasyPLL plus' system from Nanosurf. To reduce noise due to external factors, a vibration isolation platform from Minus K and an enclosure from Herzan (AEK2002) were used. 1 MHz length extension type QCRs (CX1SM) were obtained from Statek. The AFM tips (ACT-50) were purchased from AppNano.

Figure 1 shows a schematic of the electronic control and measurement instrumentation for the QCR FM-AFM. Basically a quartz crystal resonator is driven into resonance by an applied voltage. At the end of the resonating arm, an AFM tip of the desired radius is attached by a very thin layer of an adhesive. Figure 2 is a photograph of such a QCR.

When the AFM tip comes into contact with a surface, the force generated causes the resonant frequency to shift, which is measured by a phase-lock loop frequency counter. The resonant frequency of the QCR is typically 1 MHz. The relationship between frequency shift and force can be calibrated by applying force on the QCR with the light AFM cantilever. Figure 3 shows the method of calibrating the QCR. By compressing the QCR with an AFM cantilever of known compliance, the frequency shift of QCR and

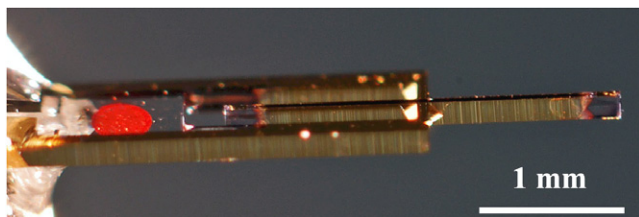


Figure 2. Photograph of the QCR. The AFM tip is at the righthand end and is about the size of the period at the end of this sentence.

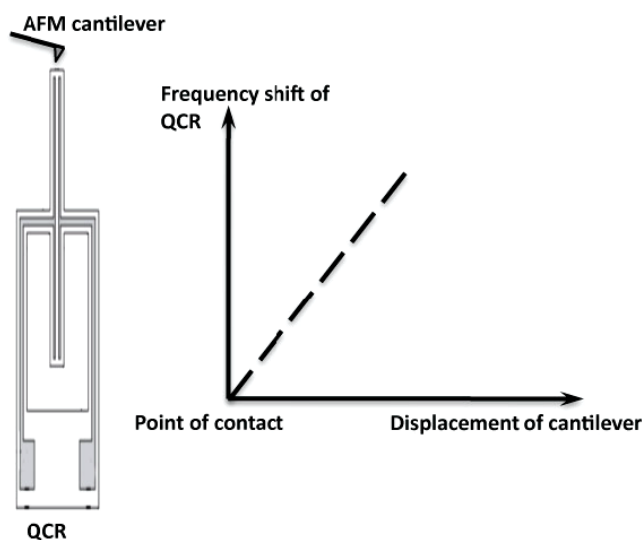


Figure 3. Method of calibrating the QCR.

corresponding displacement of the cantilever can be recorded simultaneously. The compliance of the cantilever tips is also calibrated following an established procedure [14]. At least four cantilevers with different compliances were used for calibration. A typical calibration profile using cantilevers of known compliance is given in figure 4. Good linearity between force and frequency shift is obtained. The customized QCR is attached to the AFM in place of the light cantilever. The mechanical compliance of the QCR we use is orders of magnitude lower than that of a typical AFM cantilever and can be used to apply \sim nN loads to nanostructured surfaces, e.g. for compression of a nanopillar, while maintaining adequate force and spatial resolution. It can also be used as a nanoindenter that is capable of making extremely shallow, \sim 1 nm indents. The amplitude of resonance is much less than 1 nm [15] so that the indentation tests using QCR can be considered to be a quasi-static experiment. It is therefore also useful for studying near-surface mechanical properties of soft materials including soft metallic materials and polymers.

3. Results

3.1. Calibration using materials with known properties

The AFM tip we used ranged from 5 to 46 nm in radius, which is much smaller than those used in typical nanoindentation experiments, in order to maximize lateral spatial resolution.

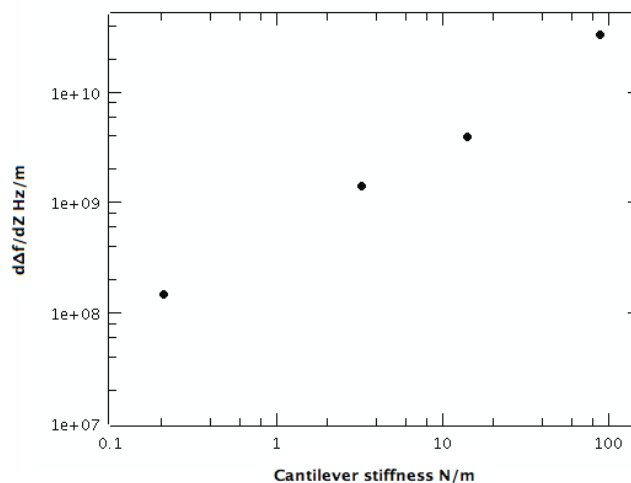


Figure 4. Typical data obtained for QCR calibration using four different AFM cantilevers of known stiffness.

Consequently, the stress sustained by the tip and the counter-surface is expected to be larger than that in a typical indenter, resulting in tip deformation and adhesion between the contacting surfaces. These considerations suggest that the oft-used Oliver–Pharr model [16] for extracting the material modulus may not be valid for our tests. We therefore needed to perform experiments on model materials with known mechanical properties that are within the measurement parameters of our instruments in order to validate a particular method of analysis. The ideal material would be a relatively low modulus elastic material whose near-surface mechanical properties are not very different from those of the bulk. Many metallic and ionic materials satisfy this requirement.

For calibration we chose several relatively soft materials: lead, sodium chloride, highly ordered pyrolytic graphite (HOPG), and three polymers. The lead (Pb) specimen used in this work was cut from a thin sheet purchased from McMaster-Carr. The surface was polished down to a 0.3 μ m polishing compound before testing at ambient condition. Sodium chloride (NaCl) specimens were cleaved from a NaCl IR window from Sigma-Aldrich. Poly(methyl methacrylate) (PMMA, $M_w \sim 177.8$ kg mol⁻¹, $M_w/M_n \sim 1.08$) was purchased from scientific polymer products, Polystyrene (PS, $M_w \sim 220.9$ kg mol⁻¹, $M_w/M_n \sim 1.03$) was purchased from a polymer source, and SU-8 was purchased from MicroChem Corp. The polymer samples were fabricated by dissolving the polymers in toluene and spin coating the polymer onto silicon substrates. The polymer films were more than 1 μ m thick and were baked above their respective T_g s overnight before running the experiments.

We performed experiments on model materials using indentation depths that ranged from 2 to about 20 nm using a 28 nm radius indenter on lead (Pb) with an oxidized surface. By assuming the Oliver–Pharr model, indentations deeper than 6 nm produced an apparent modulus in the 6 GPa range, while indentations at 2 and 4 nm produced much lower apparent moduli (figure 5). These values are much lower than what one would expect of metallic materials even if one assumes

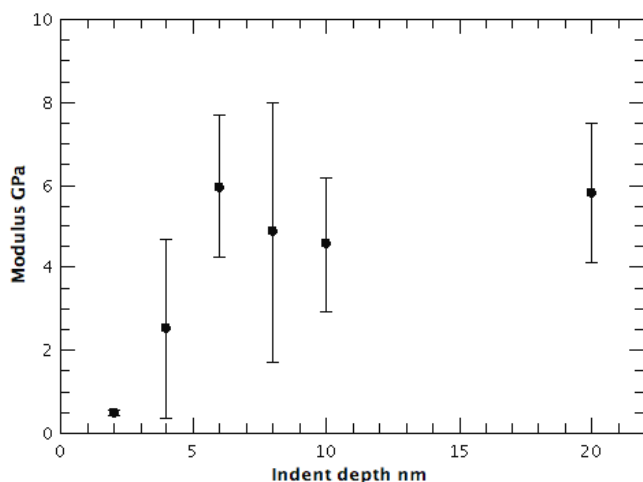


Figure 5. Apparent modulus of Pb at different indentation depths using the Oliver–Pharr Model.

that there exists an oxide layer on the surface. In this work we adopt a new approach that is an extension of the model of Lu *et al* [17] to take into account the relatively deep indentation. As shown in figure 6, by plotting the nominal compliance, i.e. force F divided by the displacement d against the displacement, the experimental data give a maximum at about $d = 0.1R$, which is consistent with the results of Lu *et al*. The nominal strain e at the maximum of the F/d curve is related to the modulus E by the equation $e = (F/\pi dER)_{\max}$, which we estimate to be 0.025–0.04 for a strain-hardening index $n = 0.1$ –0.4. By taking $(F/\pi dER)_{\max} = 0.03$ at $d = 0.1R$, the modulus $E = (F/d)_{\max}/0.03\pi R$. Figure 6 gives a schematic showing the proposed approach to obtaining modulus values.

Using the analysis described above on the indentation on Pb, we obtained an apparent modulus value of about 7 GPa for Pb by assuming that F/d_{\max} occurs at $e = 0.03$. This value is still much lower than expected for a metallic material.

Values of modulus for Pb in the literature range from 16 GPa to about 30 GPa [18]. The low apparent modulus near the surface is consistent with the existence of a thin oxide film on Pb surface. Indeed an AFM scan of the surface (figure 7) shows it to be rather rough and perhaps porous. Regardless of the chemical nature of the surface, such materials cannot be modeled by a constitutive relationship that assumes either

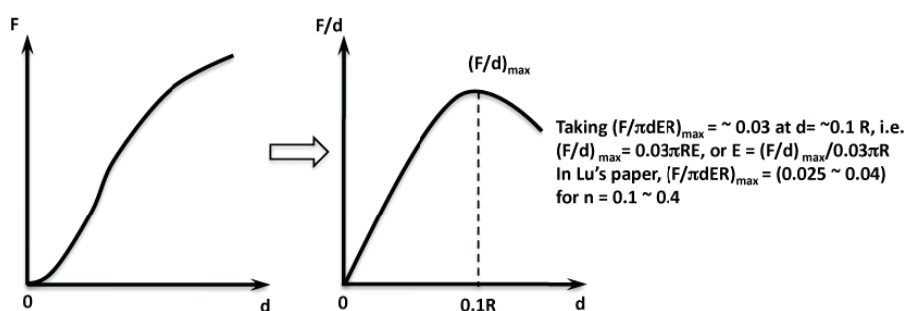


Figure 6. Schematic of the $(F/d)_{\max}$ approach to assessing modulus. Here F is the indentation load, d the indentation depth, R the tip radius, and E the Young's modulus.

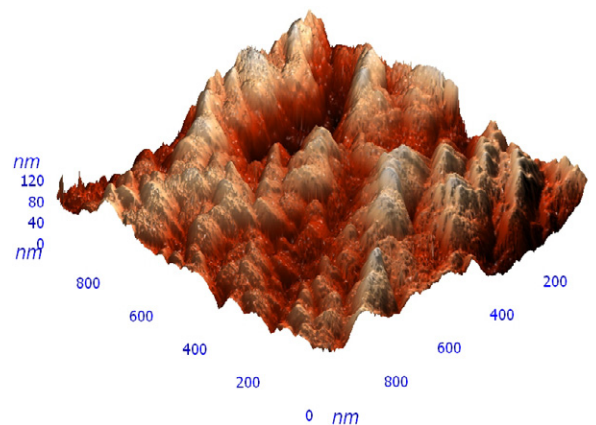


Figure 7. AFM image of polished Pb surface, which probably consists of an oxide layer rather than pure Pb.

elastic–perfectly plastic behavior or plastic hardening behavior. So it is not surprising that the measured value is so much lower than that of pure Pb.

We next carried out experiments on NaCl crystals because they are relatively low in modulus and not susceptible to contamination such as oxidation. Indentations were made on freshly cleaved NaCl surfaces. We found a significant difference between the behavior of a fresh-cleaved specimen, which was indented about 1 h after cleaving, and that of a specimen that had been left in the test chamber overnight. A specimen stored for five days exhibited an even greater difference in behavior (figure 8). The calculated apparent modulus decreases monotonically with increasing time (table 1). This systematic change is probably due to the absorption of atmospheric water because NaCl is hygroscopic. Additionally, recrystallization apparently occurred with time because AFM scans of the surface (figures 9(a), (c), and (e)) show that it changed from smooth to rough in the three specimens. Figures 9(b), (d), and (f), which are cross-sectional profiles, clearly show the difference. Nevertheless, the reported modulus of NaCl is 39.96 GPa [19], which is about 60% higher than the data we obtained from a fresh-cleaved specimen. Apparently water absorption had occurred in the period of time between cleaving the specimen and conducting the indentation experiment.

Indentation tests were also performed on HOPG, which should have few problems with oxidized layer or moisture

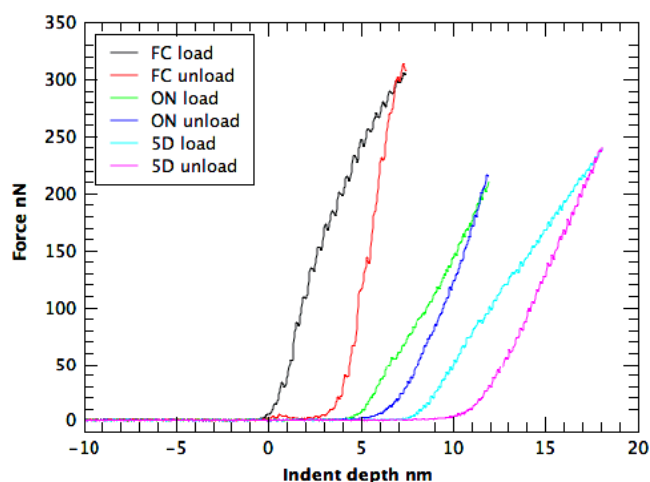


Figure 8. Representative loading and unloading indentation curves of NaCl: fresh cleaved (FC), cleaved then kept overnight (ON), and cleaved then kept for five days (5D).

effect. The indentation curves are given in figure 10. Indeed the loading and unloading curves overlap each other within the range of indentations applied, which clearly indicates that the material behaved in an elastic manner under the test conditions. The apparent modulus calculated using the Oliver–Pharr model is about 4 GPa. Using our $(F/d)_{\max}$ analysis, the modulus is from 17 to 27 GPa, which is within the range of published results, 10–36.5 GPa [20, 21].

We note that these results are given to illustrate the instrumentation and analysis and may be affected by accumulation of surface contaminants and consequent modification of the surface nanostructure. We made no attempt to control the atmosphere or humidity level. The paucity of modulus data on uncontaminated surfaces of materials for comparison is the limiting factor in our ability to further validate our instrument.

3.2. Nanoindentation of polymers

Having obtained encouraging results from the use of the QCR-AFM as an indenter on model materials, we performed nanoindentation measurements on several polymers. These results are shown in figure 11 for: (a) polystyrene, (b) poly(methyl methacrylate), and (c) SU8, a highly cross-linked epoxy often used in electronics. All three are glassy polymers at room temperature.

Again, applying our $(F/d)_{\max}$ analysis to the initial linear portions of the loading curves, we obtain modulus values of 1.2–2.0 GPa for PS, 1.4–2.3 GPa for PMMA, and 1.1–1.7 GPa for SU8. The range of calculated values results from the assumption of strain-hardening indices ranging from 0.1 to 0.4, with an index of 0.1 producing the highest moduli. Glassy polymers, such as those studied here, actually undergo significant plastic flow after yield, even in compression [22]. Thus in the flow regime a low hardening index would be appropriate if hardening does occur, as is the case with high MW polymers. Assuming a hardening index of 0.1 for all three

Table 1. Estimated modulus (GPa) of NaCl tested at various times using two methods. Tip radius = 28 nm. Loading rate = 25 nm s⁻¹.

Analysis	Modulus (GPa)			Literature
	Fresh cleaved	Overnight	5 days	
Oliver–Pharr	1.8	1.5	0.9	40
$(F/d)_{\max}$ analysis	24.8	11.3	8.50	40

polymers, the moduli calculated are 2.0 GPa for PS, 2.3 GPa for PMMA, and 1.7 GPa for SU-8. These values are consistent with data obtained from either indentation [4] or tensile test results on bulk specimens. These results cannot answer the question of whether the surface properties are different from those of the bulk because the indentations, up to about 30 nm, are large relative to the expected thickness of the surface zone. Furthermore, we do not know the hardening index of each polymer surface. Nevertheless the results are interesting and will be discussed below.

4. Discussion

In spite of the relatively deep indentation relative to the indenter radius, the loading and unloading behavior of NaCl is very similar to what one would expect from conventional nanoindentation tests, but the modulus value calculated from the $(F/d)_{\max}$ analysis is only about 60% of that of the literature value, as discussed before. On the basis of results obtained after exposure to laboratory ambient conditions for various periods of time, we surmise that moisture absorption of the specimen can lower the apparent modulus value. In the case of HOPG we did not observe plastic deformation under the test conditions. Nevertheless it was still possible to calculate the modulus, and the results fall within the range of literature values.

Before we discuss the polymer data further, we note that for the range of indentation depths attempted in this work, the force generated in the indentation of the glassy polymers is about an order of magnitude lower than those for HOPG and NaCl and other solids with covalent, ionic or metallic bonding, so features in the loading/unloading curves of the polymers have become magnified in the current graphical presentation. It is possible that the indentation behavior observed in figure 11 may not be unique to polymers.

The loading curves for all three polymers exhibit a prominent reduction in slope, i.e. softening, at an indentation depth of about 4 nm. The softening is probably associated with the onset of plastic yielding in the vicinity of the indenter³. The unloading behavior was unexpected. Instead of elastically unloading as soon as the indenter was withdrawn, the initial portion of the unloading curve had a shape close to that of the loading curve, which means that the indenter continued to be subjected to a compressive force that persisted for over 10 nm—depending on the material—after the direction of the indenter had been reversed. Yet, further along the

³ In a subsequent paper we will show that this is indeed the case.

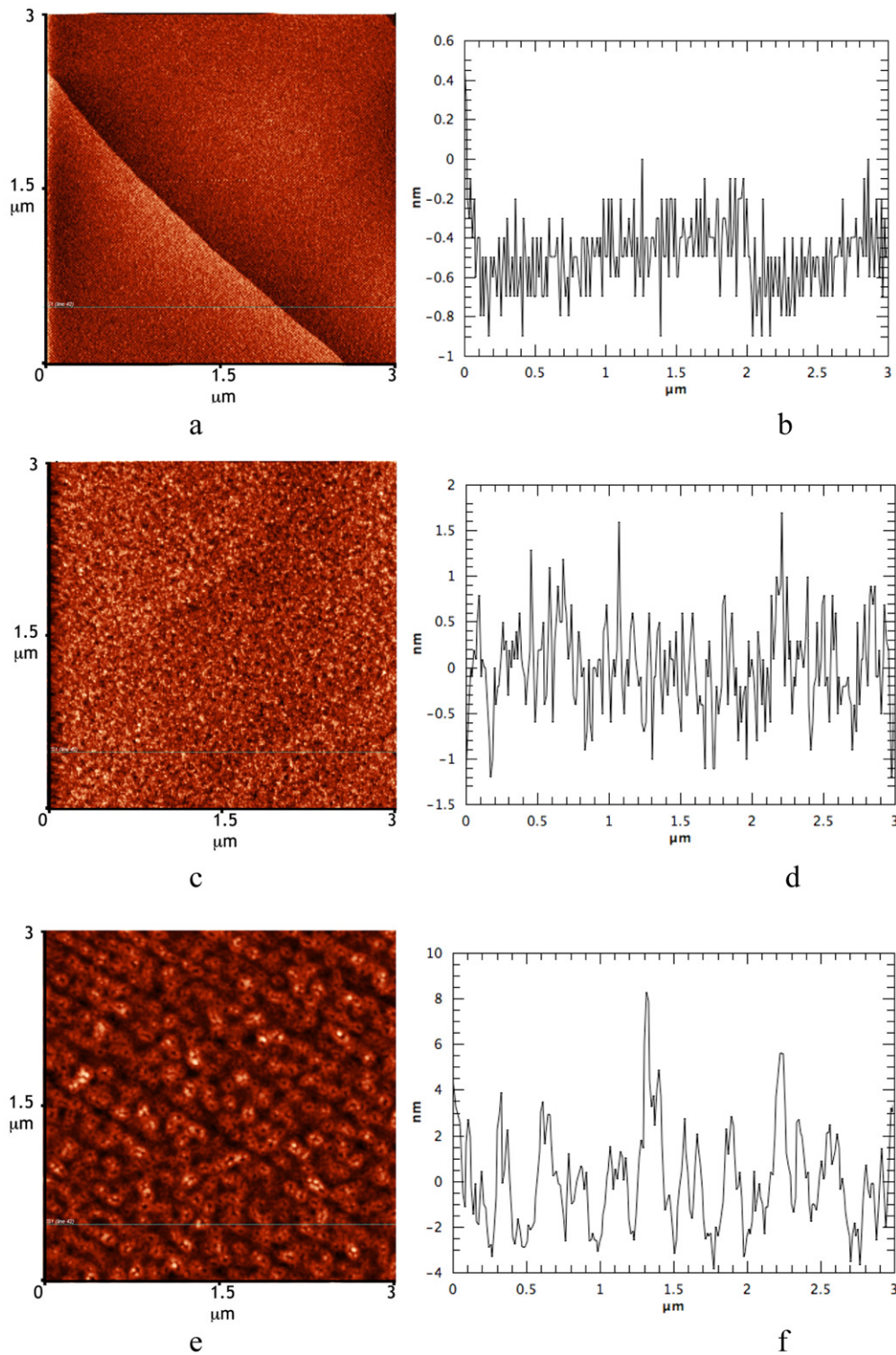


Figure 9. AFM images and corresponding cross-sectional profiles of cleaved NaCl crystals kept at ambient conditions for different time periods: (a) and (b) fresh cleaved, (c) and (d) overnight, and (e) and (f) five days. The surface became rougher with time. The cross-sectional profiles ((b), (d) and (f)) were taken from the lines marked on the AFM images.

unloading curve, the load dropped more rapidly such that the curve resembles that for an elastic–plastic material like NaCl. Consequently the polymer unloading curves can be approximated by a series combination of the unloading curves of purely elastic and elastic–plastic materials. Bearing in

mind the fact that glassy polymers elastically deform⁴ by a significant amount before the onset of plastic yielding, the

⁴ Polymer yield behavior is weakly time- or rate-dependent, and can be neglected for this discussion.

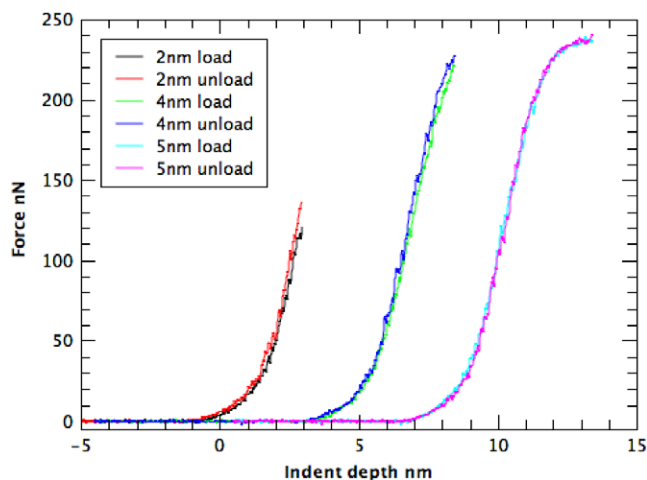


Figure 10. Representative indentation curves of HOPG.

initial part of the unloading curves of the polymers upon withdrawal of the indenter is probably due mostly to the elastic unloading of a small volume of yielded material directly underneath the indenter, and the latter part of the unloading curves is likewise due to a stronger contribution from the elastic unloading of a larger volume of material. Further experiments, which are beyond the scope of the present work, will be needed to shed light on this complex yet rich behavior.

While polymers are well known to be viscoelastic, NaCl should not exhibit significant viscoelastic behavior under the testing conditions. A simple way to determine if this is indeed the case is by varying the rate of deformation, which we did by changing the loading time from 2 to 60 s on two different NaCl specimens. The results are shown in figure 12. As expected, no significant difference can be discerned from the loading and unloading curves. These observations are consistent with the deformation behavior of single crystals of ionic compounds.

The Oliver–Pharr model is clearly not appropriate for the analysis of our results. This is in part due to the differences in the indenter geometries and that our indentations are relatively deep compared to the tip radius. The model by Lu *et al* approximates the S-shape of our loading curves better. Another analysis that does not address the geometric effect has been proposed by Fraxedas *et al* [23]. They concluded that in-plane interactions play a key role in the nanoindentation process performed with ultrasharp tips leading to a non-Hertzian response of the elastic region of the nanoindentation curve. They proposed a simple spring model to take into account the anisotropy created during the indentation process and reproduced quite well the experimental data. Due to the differences in the geometries of the indentation tips it is difficult to directly compare their results with ours, but they are generally consistent in the case of HOPG, the only material examined in both studies.

The moduli we calculated are based on the loading curves, and, except for Pb, correspond fairly closely to values in the literature. These results lend credence to our analysis, which is derived from the model by Lu *et al* [17] which uses the finite element method to simulate the deep

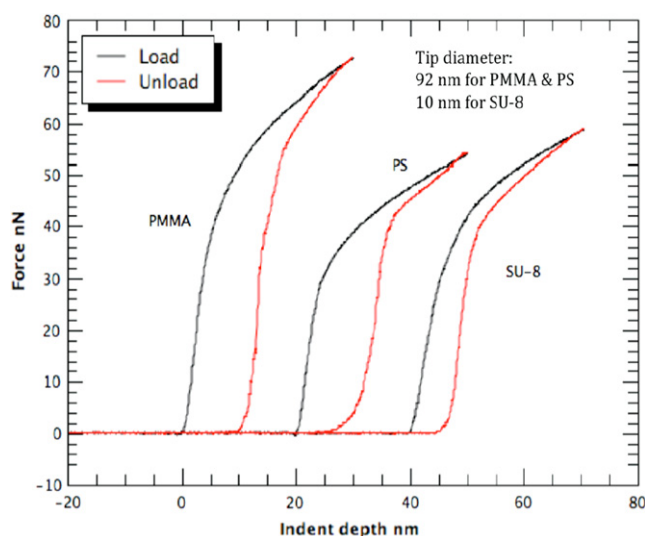


Figure 11. Deep indentation of polystyrene, poly(methyl methacrylate), and SU8, an epoxy. Indenter tip diameter was 92 nm for PS and PMMA, and 10 nm for SU-8.

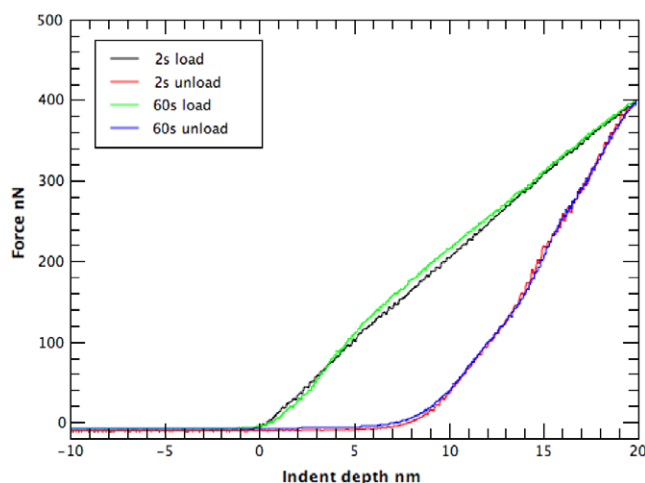


Figure 12. Indentation curves of NaCl with different loading times. The NaCl specimen was cleaved then kept in the chamber for five days before the measurement.

indentation of strain-hardening elastic-plastic materials by a rigid, spherical indenter. Their simulation results show that the ratio of the indentation load to the maximum indentation depth increases with increase of the strain-hardening index and reaches a maximum value at the maximum indentation depth of about 10% of the indenter radius. In the present experiments, such a simulation predicts that the maximum would occur at between 2 and 3 nm, which is consistent with our observations. However, their simulation assumes frictionless contact between the indenter and the specimen surface. Such an assumption, which is often made in both analytical as well as numerical simulations of indentation, is an approximation at best as adhesion of polymers to the AFM tip after indentation is a common observation, including in

the experiments described here. The analysis proposed here appears to give the most reasonable results.

One may expect that the geometry of the AFM tip would play a key role in the results. Alderighi *et al* proposed a model to take into account the tip geometry [5]. To evaluate their model, we estimated the moduli using their method, and found values about 50% higher than those obtained from the Oliver–Pharr method, which is still much lower than the bulk properties. Alderighi *et al* further noted that the apparent moduli could be much lower if the actual tip radii are larger than the nominal values provided by the manufacturers, which is typically the case [5]. In our work the indenter or tip radius is comparable to the indentation depth, therefore the differences in results observed is not a simple issue of tip radius. Simulation work on deep indentation could provide more useful information.

One of the analysis techniques used by Alderighi *et al* showed that the near-surface moduli of some amorphous polymers are comparable to or may even be higher than those of the bulk [5]. This is quite puzzling as it is expected that polymer chains on the surface are less constrained so they are more mobile and should deform more easily [24]. If true, this would suggest that the surface modulus should be lower than that of the bulk. Clearly the relationship between indent depth and modulus is dependent on the contact model used and the depth of the indent [5].

For polymers, the unloading curve will be greatly affected by not only adhesion but also viscoelastic effects. Specifically, the stress history during the loading process could play an important role on the unloading curve, which typically deviates from elastic recovery. Therefore, much work remains to be done to understand in detail elastic and plastic deformations on the polymer surface. The approach we have proposed here is to assess the modulus from the loading curve during the indentation. Thus it is expected that the stress history would produce only minor effects.

5. Conclusions and future work

A highly sensitive QCR-AFM has been demonstrated to be capable of indentations in a range of materials. We have proposed a new approach based on the loading curves to estimate the moduli of several different materials. The extracted values are, with the exception of the surface-oxidized Pb, broadly consistent with the range of published data. Future work will study nanopillars made from amorphous polymers such as PS. This will help to assess the size or surface effect on the mechanical properties.

Future work can also include extending the technique described here to hard materials. However, a different calibration procedure would be needed. The derivation of the calibration equation for the QCR-AFM is based on the assumption that the contact forces between the AFM probe tip and the surface are small. Indentations carried out on hard materials give rise to large contact forces that render the calibration curve invalid. However, it might be possible to calibrate the QCR-AFM to include the non-linear frequency to force response of the QCR. Additionally, our $(F/d)_{\max}$

analysis of the indentation curve is based on the assumption that the AFM probe tip is of a rigid material and thus the deformation of the tip is negligible. Indentations on hard materials that have moduli comparable to or larger than that of silicon (the material of choice used in manufacturing AFM probe tips) will result in deformation of the AFM probe tip. This will require a more complex analysis than the $(F/d)_{\max}$ analysis proposed here because the deformation of the probe tip cannot be neglected. We are currently working on addressing these issues to make the QCR-AFM not only suitable for soft materials but also for hard materials.

Acknowledgment

This research project is funded by NSF (CMMI-0728352).

References

- [1] Forrest J, DalnokiVeress K, Stevens J and Dutcher J 1996 Effect of free surfaces on the glass transition temperature of thin polymer films *Phys. Rev. Lett.* **77** 2002
- [2] Forrest J, DalnokiVeress K and Dutcher J 1997 Interface and chain confinement effects on the glass transition temperature of thin polymer films *Phys. Rev. E* **56** 5705
- [3] Mattsson J, Forrest J and Borjesson L 2000 Quantifying glass transition behavior in ultrathin free-standing polymer films *Phys. Rev. E* **62** 5187
- [4] Clifford C and Seah M 2005 Quantification issues in the identification of nanoscale regions of homopolymers using modulus measurement via AFM nanoindentation *Appl. Surf. Sci.* **252** 1915
- [5] Alderighi M, Ierardi V, Fuso F, Allegrini M and Solaro R 2009 Size effects in nanoindentation of hard and soft surfaces *Nanotechnology* **20** 235703
- [6] Sader J and Jarvis S 2004 Interpretation of frequency modulation atomic force microscopy in terms of fractional calculus *Phys. Rev. B* **70** 012303
- [7] Sader J, Uchihashi T, Higgins M, Farrell A, Nakayama Y and Jarvis S 2005 Quantitative force measurements using frequency modulation atomic force microscopy—theoretical foundations *Nanotechnology* **16** S94
- [8] Giessibl F 1997 Forces and frequency shifts in atomic-resolution dynamic-force microscopy *Phys. Rev. B* **56** 16010
- [9] Giessibl F and Bielefeldt H 2000 Physical interpretation of frequency-modulation atomic force microscopy *Phys. Rev. B* **61** 9968
- [10] Giessibl F 2001 A direct method to calculate tip-sample forces from frequency shifts in frequency-modulation atomic force microscopy *Appl. Phys. Lett.* **78** 123
- [11] Bottom V 1947 Note on the anomalous thermal effect in quartz oscillator plates *Am. Mineral.* **32** 590
- [12] Ratajski J 1968 Force-frequency coefficient of singly rotated vibrating quartz crystals *IBM J. Res. Dev.* **12** 92
- [13] Lee P, Wang Y and Markenscoff X 1975 High-frequency vibrations of crystal plates under initial stresses *J. Acoust. Soc. Am.* **57** 95
- [14] Cleveland J, Manne S, Bocek D and Hansma P 1993 A nondestructive method for determining the spring constant of cantilevers for scanning force microscopy *Rev. Sci. Instrum.* **64** 403
- [15] An T, Nishio T, Eguchi T, Ono M, Nomura A, Akiyama K and Hasegawa Y 2008 Atomically resolved imaging by

- low-temperature frequency-modulation atomic force microscopy using a quartz length-extension resonator *Rev. Sci. Instrum.* **79** 033703
- [16] Oliver W and Pharr G 2004 Measurement of hardness and elastic modulus by instrumented indentation: advances in understanding and refinements to methodology *J. Mater. Res.* **19** 3
- [17] Lu Y C, Kurapati S N V R K and Yang F 2008 Finite element analysis of deep indentation by a spherical indenter *J. Mater. Sci.* **43** 6331
- [18] Basaran C and Jiang J 2002 Measuring intrinsic elastic modulus of Pb/Sn solder alloys *Mech. Mater.* **34** 349
- [19] Klocek P 1991 *Handbook of Infrared Optical Materials* p 179
- [20] Enachescu M, Schleef D, Ogletree D and Salmeron M 1999 Integration of point-contact microscopy and atomic-force microscopy: application to characterization of graphite/Pt(111) *Phys. Rev. B* **60** 16913
- [21] Richter A, Ries R, Smith R, Henkel M and Wolf B 2000 Nanoindentation of diamond, graphite and fullerene films *Diamond Relat. Mater.* **9** 170
- [22] van Melick H, Govaert L and Meijer H 2003 On the origin of strain hardening in glassy polymers *Polymer* **44** 2493
- [23] Fraxedas J, Garcia-Manyes S, Gorostiza P and Sanz F 2002 Nanoindentation: toward the sensing of atomic interactions *Proc. Natl Acad. Sci. USA* **99** 5228
- [24] Fakhraei Z and Forrest J A 2008 Measuring the surface dynamics of glassy polymers *Science* **319** 600